2019 IEEE 4th Colombian Conference on Automatic Control (CCAC)
October 15-18, 2019. Diez Hotel, Medellin, Colombia.

Spacecraft Attitude Regulation in Low Earth Orbit Using Natural Torques

Camilo Riano-Rios
Mechanical and Aerospace Department
University of Florida
Gainesville-FL, U.S
crianorios@ufl.edu

Sanny Omar
Mechanical and Aerospace Department
University of Florida
Gainesville-FL, U.S
sanny.omar@ufl.edu

Riccardo Bevilacqua
Mechanical and Aerospace Department
University of Florida
Gainesville-FL, U.S
bevilr@ufl.edu

Warren Dixon
Mechanical and Aerospace Department
University of Florida
Gainesville-FL, U.S
wdixon@ufl.edu

***Abstract*—This paper presents a control algorithm for three axis attitude regulation of a 2U CubeSat by means of gravity gradient and atmospheric torques. The inertia tensor of the spacecraft is modified to keep the spacecraft in a gravity gradient stable configuration. A Lyapunov-based control law acts simultaneously to improve the pitch angle regulation performance using atmospheric torque.**

Keywords—Atmospheric torque, gravity gradient torque, attitude

I. INTRODUCTION

This paper considers the use of natural torques such as Aerodynamic Torque (AT) and Gravity Gradient Torque (GGT), with application to a 2U CubeSat that incorporates a Drag Deorbit Device (D3).

CubeSats are small spacecraft mainly used in Low Earth Orbits (LEO). At LEO, spacecraft interact with a low-density atmosphere and experience atmospheric drag. The atmospheric drag is commonly considered as a perturbation in the equations of motion for an orbiting spacecraft, but it has also been exploited to perform relative maneuvers between two or more spacecraft using differential drag (e.g., [1], [2], and [3]).

The primary purpose of a D3 device is to de-orbit a spacecraft over unpopulated areas using atmospheric drag once the orbital lifetime has finished. The D3 considered in this paper has four independent, repeatedly expandable-retractable drag surfaces used to modify the cross-wind area, mounted in the anti-ram portion of the spacecraft. Missions to perform de-orbiting and formation flying maneuvers have been designed and simulated assuming that all drag surfaces are equally deployed at all times, (cf., [4] and [5]). Since each surface is controlled independently, it is possible to experience unbalanced forces that result in torques with respect to the center of mass of the spacecraft.

Missions involving CubeSats usually require maintaining attitude for communication or sensing purposes. In [6], atmospheric torque is used in combination with magnetic torque to maintain the attitude of a 2U CubeSat within allowable ranges for sensing tasks, where a D3 like distribution of fixed drag surfaces was implemented to improve the performance of a magnetic-based attitude control. Atmospheric torques were also used in [7] to develop an adaptive sliding mode control algorithm for pitch and yaw angles, while the roll angle was controlled using different means. Roto-translational control using atmospheric drag has also been studied in results such as [8] and [9], where on-off virtual thrusters and a sliding mode controller, respectively, were developed through a Lyapunov analysis.

The study of spacecraft attitude dynamics based on natural torques is heavily dependent on the spacecraft physical design. The distribution and degrees of freedom of the drag surfaces directly affect the capability of the spacecraft to control or stabilize its attitude. Common designs allow two degrees of freedom for each drag surface, e.g expand/retract and rotation about an axis, which results in increased complexity and more moving parts, both undesirable for real operation.

In this work, we design a controller to regulate the attitude of the spacecraft using a D3 device that provides one degree of freedom for each one of its four drag surfaces. The atmospheric and gravity gradient torques are included in the dynamic model and are used as means to stabilize the CubeSats attitude. The use of natural torques to regulate the attitude of a spacecraft represents a challenge due to the limited amplitude of these torques, necessitating the design of a controller that considers input saturation. Moreover, the integration of GGT and AT for three axis attitude regulation is also challenging due to their mutual dependence, i.e. changing a drag surface's cross-sectional area to vary the experienced drag force also changes the inertia tensor and vice versa. This paper presents the development of a saturated controller through a Lyapunov analysis for pitch regulation. Then, the numerical solution to a minimization problem with nonlinear constraints is used to integrate this controller with stabilization by GGT and achieve asymptotic convergence of the three attitude angles.

II. BACKGROUND

This section presents the problem statement followed by the definition of AT and GGT. A simplified version of a particular design of the D3 device is also presented here.

A. Drag Deorbit Device (D3)

This paper considers a D3 device designed to be self-contained and attachable to standard CubeSats. It is installed in the anti-ram face of the spacecraft and has four drag surfaces each offset by 90 degrees with fixed inclination of 20 degrees with respect to the anti-ram face of the spacecraft. The drag surfaces are rolled from $0.0762\ mm$ thick Austenitic 316 stainless steel stock, each surface is attached to a drum that is driven by a stepper motor. The width and length of the drag surfaces are $40\ mm$ and $3.7\ m$ respectively, and the maximum

978-1-5386-6962-4/19/$31.00 ©2019 IEEE

Authorized licensed use limited to: Florida Institute of Technology. Downloaded on March 03,2025 at 15:46:48 UTC from IEEE Xplore. Restrictions apply.

total cross-wind area is approximately $0.5m^2$. The 20 degrees fixed inclination of the drag surfaces allow the spacecraft to have its center of pressure always behind the body of the spacecraft, which results in ram alignment. Due to construction tolerances and error in the deployment level of each drag surface, the total torque with respect to the center of mass of the spacecraft is uncertain, resulting in undesired oscillations and even possible instability. Moreover, in most operation cases the spacecraft is required to have one face pointing to the Earth for communication or sensing purposes.

B. Coordinate Systems

The orbital reference frame (O) shown in Fig. 1 and its attached coordinate system are defined as follows. The origin is located at the center of mass of the spacecraft, the $\hat{o}_3$ axis points from the center of the Earth to the spacecraft center of mass, the $\hat{o}_2$ axis is aligned with the orbit angular momentum vector and the $\hat{o}_1$ axis completes a right-hand Cartesian coordinate system. The body reference frame (B) is attached to the spacecraft's body, its coordinate system is centered at the spacecraft's center of mass and is aligned with the body's principal axes of inertia. The drag surfaces DS1 through DS4 are also shown in Fig. 1.

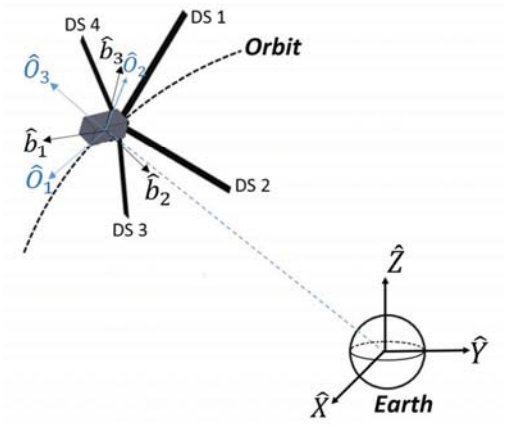

Fig. 1 Inertial, orbit and body Coordinate systems definition

C. Problem Description

The Advanced Autonomous Multiple Spacecraft (ADAMUS) laboratory at University of Florida has been conducting research on the use of natural forces for orbit maneuvering purposes, such as de-orbiting and formation flying. The D3 device has been conceived based on the experience acquired from previous research and designs to take advantage of the aerodynamic drag in CubeSat missions.

Inexpensive and simple means to stabilize attitude are preferable in CubeSats. The configuration of the drag surfaces in the D3 device allows the spacecraft to remain aligned with the direction of motion (ram aligned) once they are deployed. Once the spacecraft is released into orbit, it needs to be de-tumbled to deploy its drag panels. This stage is assumed to be completed using magnetic torques and is beyond the scope of this work. For more details regarding de-tumbling strategies, see, for example [3].

Once the drag surfaces are deployed and the spacecraft is ram aligned, it is important to ensure that the spacecraft's attitude is suitable for communication and/or sensor pointing within reasonable levels of accuracy about each of the body axes. Using natural torques for this purpose results in power and propellant saving and increase in the payload availability.

D. Atmospheric Torque

For a spacecraft orbiting in LEO, atmospheric drag is the largest non-gravitational force. In LEO, the atmosphere can be considered as an interaction with a rarefied gas instead of a continuous flow. The rarefied particle interaction with each drag surface is assumed to produce specular reflection. The resulting drag force $\vec{F}_D$ is

$$\vec{F}_D = -\frac{1}{2} C_D \rho \frac{A}{m} v_\perp^2 \hat{v}_\perp \tag{1}$$

where C_D is the drag coefficient, ρ is the atmospheric density, A and m are the drag surface's area and spacecraft's mass respectively, $v_\perp$ is the component of the spacecraft's velocity relative to the atmosphere that is perpendicular to the drag surface, and $\hat{v}_\perp$ is the unit vector in the direction of $\vec{v}_\perp$. The atmospheric density ρ is the main source of uncertainty for the drag force. Although there are several models for the atmospheric density, it is known that the solar and geomagnetic activity produce changes that are difficult to model and predict. Therefore, most of the available models are empirical.

The assumption of specular reflection allows the force produced by atmospheric drag to be modeled as a single force applied at the geometric center of the deployed portion of each drag surface. Therefore, by having different deployment levels of opposite drag surfaces, it is possible to create atmospheric torque with respect to the center of mass of the spacecraft.

Assuming that the spacecraft is in a circular orbit, the velocity vector of the spacecraft with respect to the atmosphere $\vec{v}_r$ is defined in the orbit reference frame as

$$\vec{v}_r = \begin{bmatrix} 1 \\ 0 \\ 0 \end{bmatrix} v_r \tag{2}$$

and in the body reference frame as

$$\vec{v}_r = C_{BO} \begin{bmatrix} 1 \\ 0 \\ 0 \end{bmatrix} v_r = \begin{bmatrix} c\theta c\psi \\ s\phi s\theta c\psi - c\phi s\psi \\ c\phi s\theta c\psi + s\phi s\psi \end{bmatrix} v_r \tag{3}$$

where C_{BO}, defined as

$$C_{BO} = \begin{bmatrix} c\theta c\psi & c\theta s\psi & -s\theta \\ s\phi s\theta c\psi - c\phi s\psi & s\phi s\theta s\psi + c\phi c\psi & s\phi c\theta \\ c\phi s\theta c\psi + s\phi s\psi & c\phi s\theta s\psi - s\phi c\psi & c\phi c\theta \end{bmatrix} \tag{4}$$

is the direction cosine matrix from the orbit to the body reference frame using a 3-2-1 Euler angles rotation sequence, the angles ϕ, θ, ψ are called roll, pitch and yaw respectively, where $c(\cdot) = \cos(\cdot)$ and $s(\cdot) = \sin(\cdot)$.

The unit vector $\hat{v}_\perp$ for the drag surface labeled as DS1 in Fig. 1 is defined in the body frame as $\hat{v}_{\perp,1} = [c20°, 0, s20°]^T$. The

Authorized licensed use limited to: Florida Institute of Technology. Downloaded on March 03,2025 at 15:46:48 UTC from IEEE Xplore. Restrictions apply.

magnitude of $\vec{v}_r$ along the direction $\hat{v}_{\perp,1}$ is given by $v_{\perp,1} = \vec{v}_r \cdot \hat{v}_{\perp,1}$, then

$$v_{\perp,1} = \big(c20°c\theta c\psi + s20°(c\phi s\theta c\psi + s\phi s\psi)\big)v_r. \quad (5)$$

Similarly, we can obtain the normal components for each drag surface

$$v_{\perp,2} = \big(c20°c\theta c\psi + s20°(s\phi s\theta c\psi - c\phi s\psi)\big)v_r \quad (6)$$

$$v_{\perp,3} = \big(c20°c\theta c\psi - s20°(c\phi s\theta c\psi + s\phi s\psi)\big)v_r \quad (7)$$

$$v_{\perp,4} = \big(c20°c\theta c\psi - s20°(s\phi s\theta c\psi - c\phi s\psi)\big)v_r. \quad (8)$$

To compute each torque, the drag force $\vec{F}_d$ for each surface can be obtained from (1) and the resulting torque is evaluated as

$$\vec{\tau}_{d,i} = \vec{r}_i \times \vec{F}_{d,i}\ , i = 1,2,3,4 \quad (9)$$

where the vector $\vec{r}_i$ points from the spacecraft center of mass to the geometric center of the i^{th} drag surface and is expressed in the body coordinate system. Finally, the total torque due to atmospheric drag is

$$\vec{\tau}_d = \sum_{i=1}^{4} \vec{\tau}_{d,i}\ . \quad (10)$$

E. Gravity Gradient Torque

Considering the spacecraft as a rigid body in space and evaluating how strong the gravity forces are along the body, the parts of the spacecraft that are closer to the Earth will experience stronger gravitational attraction than those that are further, creating a gradient of gravitational force along the body of the spacecraft. This gradient produces a torque about the center of mass that depends on its attitude.

The gravity gradient torque is a natural free attitude stabilization method due to its properties at certain attitude configurations. The expression for the gravity gradient torque, is [10]

$$\vec{\tau}_{GG} = \frac{3GM_\oplus}{R_c^5}\vec{R}_c \times I\vec{R}_c, \quad (11)$$

where $\vec{R}_c$ is the vector that goes from the center of the Earth to the center of mass of the spacecraft, $M_\oplus$ is the mass of the Earth, G is the universal gravitational constant and $I = diag(I_1, I_2, I_3)$ is the inertia matrix of the spacecraft. The expression for $\vec{R}_c$ in the body frame, is

$$\vec{R}_c = \begin{bmatrix} R_{c1} \\ R_{c2} \\ R_{c3} \end{bmatrix} = C_{BO}\begin{bmatrix} 0 \\ 0 \\ R_c \end{bmatrix}. \quad (12)$$

Based on the assumption that the body frame is aligned with the principal axes of inertia of the spacecraft, the gravity gradient torque in the body frame is

$$\vec{\tau}_{GG} = \frac{3GM_\oplus}{R_c^5}\begin{bmatrix} R_{c2}R_{c3}(I_3 - I_2) \\ R_{c1}R_{c3}(I_1 - I_3) \\ R_{c1}R_{c2}(I_2 - I_1) \end{bmatrix}. \quad (13)$$

III. Attitude Dynamics

In this section, we will consider a 2U CubeSat that uses the D3 device to produce AT and GGT. Considering the features of the D3 device and its range of operation, a 3-2-1 Euler sequence is used to parameterize the attitude.

A. Equations of Motion

The spacecraft attitude dynamics can be represented as

$$I\dot{\vec{\omega}} + \tilde{\omega}I\vec{\omega} = \vec{\delta} \quad (14)$$

where $\vec{\omega} = \left[\omega_x, \omega_y, \omega_z\right]^T$ is the angular velocity of the spacecraft with respect to the inertial reference frame, and $\vec{\delta}$ is the vector containing torques commonly considered as disturbances, such as AT and GGT, where $\tilde{\omega}$ is the skew-symmetric matrix defined as

$$\tilde{\omega} = \begin{bmatrix} 0 & -\omega_z & \omega_y \\ \omega_z & 0 & -\omega_x \\ -\omega_y & \omega_x & 0 \end{bmatrix}. \quad (15)$$

In the case of a CubeSat with an attached D3 device, the term $\vec{\delta} = \vec{\tau}_d + \vec{\tau}_{GG}$ in (14) contains the AT ($\vec{\tau}_d$) and GGT ($\vec{\tau}_{GG}$) from (10) and (13) respectively.

B. Modeling Assumptions

The following development assumes the spacecraft is on a circular LEO orbit. This assumption is reasonable considering that a common orbit for CubeSats is that of the International Space Station (ISS), which is circular. The development also assumes that ϕ, θ and ψ are small angles, to simplify the expression for the GGT and subsequent stability analysis.

Based on the circular LEO orbit assumption, the angular velocity of the orbit frame with respect to the inertial frame Ω can be expressed in the orbit coordinate system as

$$\vec{\omega}_{O/I} = \Omega\hat{o}_2 \quad (16)$$

where the angular velocity is constant, and its magnitude is

$$\Omega = \sqrt{\frac{GM_\oplus}{R_c^3}}. \quad (17)$$

The vector $\vec{\omega}$ in (14) represents the angular velocity of the spacecraft's body with respect to the inertial reference frame, given by

$$\vec{\omega} = \vec{\omega}_{B/O} + \vec{\omega}_{O/I} \quad (18)$$

where $\vec{\omega}_{B/O}$ is the angular velocity of the body frame with respect to the orbit frame. In the body coordinate system, and using the 3-2-1 Euler angles sequence kinematics, this vector can be written as

$$\vec{\omega}_{B/O} = \begin{bmatrix} -s\theta & 0 & 1 \\ s\phi c\theta & c\phi & 0 \\ c\phi c\theta & -s\phi & 0 \end{bmatrix}\begin{bmatrix} \dot{\psi} \\ \dot{\theta} \\ \dot{\phi} \end{bmatrix}. \quad (19)$$

Using the direction cosine matrix C_{BO} in (4) to (16), $\vec{\omega}$ can be expressed in the body coordinated system as

Authorized licensed use limited to: Florida Institute of Technology. Downloaded on March 03,2025 at 15:46:48 UTC from IEEE Xplore. Restrictions apply.

$$\vec{\omega} = \begin{bmatrix} \dot{\phi} - s\theta\dot{\psi} + \Omega c\theta s\psi \\ s\phi c\theta\dot{\psi} + c\phi\dot{\theta} + \Omega(s\phi s\theta s\psi + c\phi c\psi) \\ c\phi c\theta\dot{\psi} - s\phi\dot{\theta} + \Omega(c\phi s\theta s\psi - s\phi c\psi) \end{bmatrix}. \quad (20)$$

Applying the small angle assumption, (20) can be approximated as

$$\vec{\omega} \approx \begin{bmatrix} \dot{\phi} + \Omega\psi \\ \dot{\theta} + \Omega \\ \dot{\psi} - \Omega\phi \end{bmatrix} \Rightarrow \dot{\vec{\omega}} \approx \begin{bmatrix} \ddot{\phi} + \Omega\dot{\psi} \\ \ddot{\theta} \\ \ddot{\psi} - \Omega\dot{\phi} \end{bmatrix}, \quad (21)$$

where $\dot{\vec{\omega}}$ is the angular acceleration approximated with the small angles assumption.

The GGT expression in (13) can be simplified using the circular LEO orbit and the small angle assumptions. The resulting GGT is expressed in the body coordinate system as

$$\vec{\tau}_{GG} \approx 3\Omega^2 \begin{bmatrix} (I_3 - I_2)\phi \\ -(I_1 - I_3)\theta \\ 0 \end{bmatrix}. \quad (22)$$

Substituting (21) and (22) into (14), yields the following system that describes the attitude dynamics [10]

$$\begin{gathered} I_1\ddot{\phi} + \Omega(\mathrm{I}_1 - \mathrm{I}_2 + \mathrm{I}_3)\dot{\psi} + 4\Omega^2(I_2 - I_3)\phi = \tau_{d1} \\ I_2\ddot{\theta} + 3\Omega^2(I_1 - I_3)\theta = \tau_{d2} \\ I_3\ddot{\psi} + \Omega(I_2 - I_1 - I_3)\dot{\phi} + \Omega^2(I_2 - I_1) = \tau_{d3}. \end{gathered} \quad (23)$$

C. Change of Inertia Tensor Due to Changes in the Drag Surfaces

From (22) it is possible to vary the GGT by changing the inertia tensor I. In fact, there are configurations of the inertia tensor where the linearized equations of motion are stable due to the GGT.

The drag surfaces available in the D3 device can be used to produce a GGT stable configuration of the inertia tensor. To compute the inertia tensor, the spacecraft is considered as an assembly of multiple rigid bodies with their own inertia tensors. The 2U body of the spacecraft is assumed to be a rectangular box with mass of 1.5 kg. Each drag surface is composed of two rigid bodies: one flat rectangular plate (deployed portion), and one thick-walled cylinder (rolled portion).

The dimensions of each rigid body change depending on the deployment level of the drag surface, changing the inertia tensor of each body. In the case of the flat panel, the length of one of its sides represents the drag surface's deployed length. The thin cylinder changes its radius depending on the rolled portion of the drag surface.

To calculate the inertia tensor for the entire spacecraft, each inertia tensor needs to be computed with respect to the spacecraft's center of mass. For this calculation, each inertia matrix is required to be aligned with the CubeSat's body axes. The inertia tensor of each flat plate $I^*_{fp,i}$ needs to be rotated using

$$I_{fp,i} = R_{fp,i}\, I^*_{fp,i}\, R^T_{fp,i}\ , i = 1,2,3,4. \quad (24)$$

where the rotation matrix $R_{fp,i}$ aligns the principal axes of the i^{th} flat plate with the body axes of the spacecraft. No rotation is required for the thin cylinders due to their geometry and how they are mounted on the spacecraft. The parallel axis theorem to compute the inertia tensor of each body with respect to the spacecraft's center of mass using

$$I_b^{com} = I_b + I_{PA}, \quad (25)$$

where I_b is the inertia tensor of the body of interest, and the matrix I_{PA}

$$I_{PA} = \begin{bmatrix} m_b(\bar{b}_2{}^2 + \bar{b}_3{}^2) & -m_b(\bar{b}_1\bar{b}_2) & -m_b(\bar{b}_1\bar{b}_3) \\ -m_b(\bar{b}_1\bar{b}_2) & m_b(\bar{b}_1{}^2 + \bar{b}_3{}^2) & -m_b(\bar{b}_2\bar{b}_3) \\ -m_b(\bar{b}_1\bar{b}_3) & -m_b(\bar{b}_2\bar{b}_3) & m_b(\bar{b}_1{}^2 + \bar{b}_2{}^2) \end{bmatrix}, \quad (26)$$

applies the parallel axis theorem to that body. In (26), m_b, $\overline{b_1}$, $\overline{b_2}$ and $\overline{b_3}$ represent the mass of the body of interest, and the distances from the spacecraft's center of mass to the body's center of mass along $\hat{b}_1$, $\hat{b}_2$ and $\hat{b}_3$ respectively. The location of the spacecraft's center of mass is also affected by the deployment level of the drag surfaces. Therefore, it is important to determine its location prior to the computation of the inertia tensor and atmospheric torque.

IV. Control Design

This section presents the design of a controller to stabilize the CubeSat's attitude using natural torques. The GGT and AT are combined such that the roll and yaw angles are regulated to zero using GGT and the pitch regulation performance is improved using a Lyapunov-based bounded control law that uses the AT to regulate the modified state

$$r = \theta + \alpha\dot{\theta}, \quad (27)$$

where $\alpha \in \Re$ is a constant positive gain.

A. Gravity Gradient Stability

The assumption of small angles is useful to study the stability of the system using gravity gradient torque. This assumption is also reasonable considering the fact that the D3 device's configuration passively seeks to keep the spacecraft ram aligned. To study the influence of GGT on the stability of the system in (23) we can set the AT to be zero and then apply the stability analysis for linear systems. From this analysis, the well-known gravity gradient stable configuration of the inertia tensor to remain stable can be obtained as [10]

$$I_2 \geq I_1 \geq I_3. \quad (28)$$

If (28) is satisfied, the body frame will tend to be aligned with the orbit frame due to the action of GGT. A control algorithm to deploy all drag surfaces considering this condition is developed in the next subsections.

B. Atmospheric Torque for Attitude Regulation

The condition in (28) requires the GGT to be the only torque acting on the system. Due to the coupling between roll and yaw and considering that the AT only has components on the $\hat{b}_2$ and $\hat{b}_3$ axes, we set $\tau_{d3} = 0$ to stabilize the roll and yaw angles using only GGT and develop a Lyapunov based controller to use the τ_{d2} component of the AT to improve performance in stabilization of the pitch dynamics. The AT depends on the spacecraft's attitude, so the drag surfaces DS2 and DS4 need to

Authorized licensed use limited to: Florida Institute of Technology. Downloaded on March 03,2025 at 15:46:48 UTC from IEEE Xplore. Restrictions apply.

vary their deployment levels in time to ensure that $\tau_{d3} = 0$ if the attitude angles are not zero. Although the pitch dynamics in (23) seem linear, it is important to note that the inertia tensor is not constant and the magnitude of the atmospheric is very limited. Since the goal is to develop a control law that uses the atmospheric torque τ_{d2} to contribute for attitude stabilization, then input saturation and the variation of the inertia tensor must be considered in the stability analysis. In an operational case of a CubeSat with the D3 device, once the spacecraft is detumbled and the drag surfaces are initially deployed, small perturbation torques are induced due to small differences in the deployment level for each pair of opposite drag surfaces. Moreover, missions that involve the CubeSats with a mounted D3 device will use it for orbit maneuvering, requiring active variation of the total drag surface area. These maneuvers will also contribute to generate perturbation torques because each drag surface is commanded individually. Undesired torques generate orientation and angular velocity errors that need to be compensated and ensuring stability by GGT may not be enough in cases where considerable angular velocities are induced.

Based on the pitch dynamics in (23) and on the subsequent stability analysis, we design the torque control input on the second body axis $\hat{b}_2$ as follows

$$\tau_{d2} = \left(-K\, tanh\, r + \left(\frac{3\Omega^2(I_1 - I_3)}{I_2} - \frac{1}{\alpha^2}\right)\theta - \frac{1}{\alpha}\dot{\theta}\right) I_2 \tag{29}$$

Where r is defined in (27) and $K \in \Re$ is a constant positive gain.

Theorem 1: Given the pitch dynamics in (23) and its corresponding assumptions, the controller in (29) yields global asymptotic pitch regulation in the sense that

$$\lim_{t\to\infty} |\theta|\ , \left|\dot{\theta}\right| \to 0. \tag{30}$$

Proof: To prove theorem 1, we first define the positive definite candidate Lyapunov function

$$\mathrm{V(t)} = \frac{1}{2}\theta^2 + \frac{1}{2}r^2, \tag{31}$$

The time derivative of (31) is

$$\dot{V} = \frac{1}{\alpha}(\theta r - \theta^2) + r\left(\dot{\theta} + \alpha\ddot{\theta}\right). \tag{32}$$

Substituting the pitch dynamics in (23) for $\ddot{\theta}$, substituting (29) for τ_{d2} and cancelling common terms yields

$$\dot{V} = -\frac{1}{\alpha}\theta^2 - K\alpha\, r \tanh r, \tag{33}$$

which can be upper bounded as [11]

$$\dot{V} \leq -\frac{1}{\alpha}\theta^2 - K\alpha \tanh^2 r. \tag{34}$$

Since $\dot{V}$ is negative definite, then $\theta, \dot{\theta} \in \mathcal{L}_\infty$. Moreover, since $\Omega, \mathrm{I}_1, I_2, I_3 \in \mathcal{L}_\infty$ by assumption, then the controller in (29) is also bounded. From (32), $\theta, \tanh r \in \mathcal{L}_2$ then by Barbalat's lemma

$$\lim_{t\to\infty} |\theta|, |\tanh r| \to 0, \tag{35}$$

then $|r| \to 0$ and $\left|\dot{\theta}\right| \to 0$.

C. Integration of GGT and AT for Attitude Regulation

The inertia tensor I and the AT are functions of the drag surfaces' deployment levels. To integrate the controller presented in (29) with the GGT stability condition of (28), additional efforts are required. The control algorithm is required to provide the spacecraft with the deployment level for each drag surface at each time step. Our proposed approach consists in ensuring the GGT stability condition and then finding a good approximation to the AT required by the control law (*29*). The formulation of a minimization problem can be written as

$$\min_{L} \left\|\vec{\tau}_d - \vec{\tau}_{d,des}\right\| \ s.t \begin{cases} 0 \leq L_i \leq 3.7m\ , i = 1,2,3,4 \\ \dfrac{I_1}{I_2} - 1 \leq 0 \\ \dfrac{I_3}{I_1} - 1 \leq 0 \end{cases} \tag{36}$$

where $L = [L_1, L_2, L_3, L_4]^T$ is the vector containing the deployment level of each drag surface, and $\vec{\tau}_{d,des} \in \Re^3$ is the desired AT which includes the controller in (29). This minimization problem with nonlinear constraints is solved using the 'fmincon' function in MATLAB. However, it is not guaranteed that a global minimum is achieved at each time step.

V. Simulation Results

Numerical simulations were performed to test the controller's performance. Integration of the nonlinear attitude equations of motion was performed using the MATLAB's variable step ODE45 algorithm. The spacecraft is simulated in equatorial circular orbit with altitude $335km$, J_2 perturbation and variable atmospheric density obtained from the Harris-Priester model [12]. Note that the control inputs obtained from Eq. (36) are computed every minute using a constant estimate of the atmospheric density $\rho = 6.98 \times 10^{-12}\ kg/m^3$.

TABLE I Initial Conditions

$\boldsymbol{\phi_0}$	$\boldsymbol{\theta_0}$	$\boldsymbol{\psi_0}$	$\dot{\boldsymbol{\phi}}_{\mathbf{0}}$	$\dot{\boldsymbol{\theta}}_{\mathbf{0}}$	$\dot{\boldsymbol{\psi}}_{\mathbf{0}}$
$5\ deg$	$10\ deg$	$-6\ deg$	$-0.03\ deg/s$	$0.07\ deg/s$	$0.05\ deg/s$

A. Open Loop Simulations

These simulations evaluate the system's performance in open loop operation considering two different cases and the initial conditions presented in Table 1. The first case considers that all drag surfaces are equally deployed $3m$ during the entire maneuver, while in the second case the drag surfaces are deployed in such a way that the stability condition (28) is satisfied by making $L_1 = L_3 = 3m$ and $L_2 = L_4 = 1.5m$.

Fig. 2 presents the resulting attitude angles for both cases. In the first case (left) the CubeSat remains ram aligned with bounded oscillations in pitch and yaw angles. Nevertheless, the roll angle increases indefinitely meaning that the spacecraft is spinning over the $\hat{b}_1$ axis. On the other hand, the simulation for the second case shows that all three angles remain bounded when the condition (28) is met, but they do not converge to zero due to the action of the attitude dependent AT. Results for the second simulation are also shown in Fig. 2 (right).

Authorized licensed use limited to: Florida Institute of Technology. Downloaded on March 03,2025 at 15:46:48 UTC from IEEE Xplore. Restrictions apply.

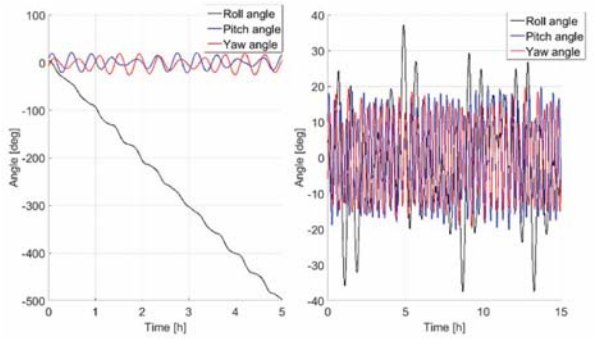

Fig. 2 Results for open loop simulations

B. *Closed Loop Simulations*

In the closed loop simulations two cases are also considered. First, the GGT stability is ensured by solving (36), and the desired AT is set to $\vec{\tau}_{d,des} = [0,0,0]^T$ to compensate for the variation in AT due to the spacecraft's attitude. For the second simulation case, the Lyapunov-based controller from (29) is included in the second component of the $\vec{\tau}_{d,des}$ vector to solve (36). The closed loop simulations have the same initial conditions shown in Table 1 except for the initial pitch $\theta_0 = 15deg$ and pitch rate $\dot{\theta}_0 = 0.25\ deg/s$ which are modified to validate the performance improvement provided by the controller (29). The resulting attitude angles for the first and second simulation are shown in Fig. 3 as dashed and solid lines respectively.

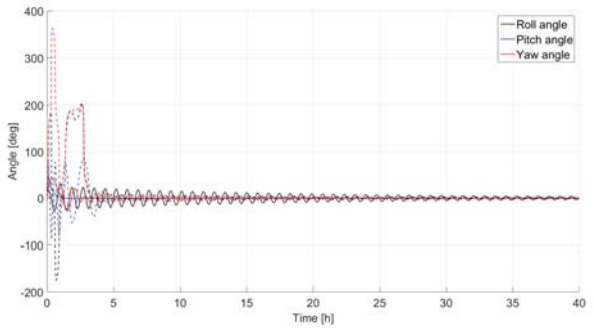

Fig. 3 Attitude angles for closed loop simulations

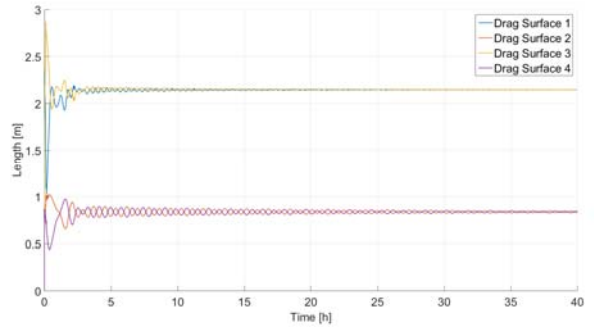

Fig. 4 Control commands using Lyapunov controller

Although both algorithms asymptotically stabilize the spacecraft's attitude, the angle profiles obtained without including the Lyapunov-based controller are not physically feasible for the D3 device. By including the controller (29), the CubeSat is successfully stabilized without unfeasible orientations for the D3. The control commands for the simulation implementing (29) and (36) are shown in Fig. 4.

VI. CONCLUSION

A novel control algorithm to stabilize the attitude of a 2U CubeSat using the D3 device is developed. The controller exploits the gravity gradient and atmospheric torques to keep the spacecraft's body aligned with the orbit frame by changing the level of deployment of four drag surfaces. Improved performance has been achieved compared with using only GGT by including a Lyapunov-based bounded controller for the pitch angle regulation. Simulations have shown that the controller is robust to small uncertainty in the atmospheric density. Additional preliminary simulations were performed and have shown sensitivity to the location of the center of mass. Therefore, improvements to overcome reasonable levels of uncertainty in this parameter are required. Future efforts will consider estimation of time-varying atmospheric density and the integration of attitude stabilization with missions where drag-based orbital maneuvering is also required.

References

[1] C. L. Leonard, W. M. Hollister and E. V. Bergmann, "Orbital Formationkeeping with Differential Drag," *Journal of Guidance, Control and Dynamics,* pp. 108-113, 1989.

[2] R. Bevilacqua and M. Romano, "Rendezvous Maneuvers of Multiple Spacecraft Using Differential Drag Under J2 Perturbation," *Journal of Guidance, Control and Dynamics,* vol. 31, no. 6, pp. 1595-1607, 2008.

[3] D. Guglielmo, S. Omar and R. Bevilacqua, "Drag Deorbit Device: A new Standard Reentry Actuator for CubeSats," *Journal of Spacecraft and Rockets,* vol. 56, no. 1, pp. 129-145, 2019.

[4] C. Riano-Rios, R. Bevilacqua and W. E. Dixon, "Relative Maneuvering for Multiple Spacecraft Via Differential Drag Using LQR and Constrained Least Squares," in *29th AAS/AIAA Space Flight Mechanics Meeting*, Ka'anapali-HI, U.S, 2019.

[5] S. Omar, D. Guglielmo and R. Bevilacqua, "Drag De-orbit Device (D3) Mission for Validation of Controlled Spacecraft Re-entry Using Aerodynamic Drag," in *IAA Cubesat Conference* , Rome, Italy, 2017.

[6] R. Sutherland, I. Kolmanovsky and A. R. Girard, "Attitude Control of a 2U CubeSat by Magnetic and Air Drag Torques," *IEEE Transactions on Control Systems Technology* , p. Article in Press, 2018.

[7] Z. Hao, Orbital Aerodynamic Attitude Control, Manchester, UK: University of Manchester, 2018.

[8] M. Pastorelli, R. Bevilacqua and S. Pastorelli, "Differential-Drag-based roto-translational control for propellant-less spacecraft," *Acta Astronautica,* vol. 114, pp. 6-21, 2015.

[9] R. Sun, J. Wang, Z. Dexin, Q. Jia and X. Shao, "Roto-Translational Spacecraft Formation Control Using Aerodynamic Forces," *Journal of Guidance, Control and Dynamics,* vol. 40, no. 10, pp. 2556-2568, 2017.

[10] H. Schaub and J. L. Junkins, Analytical Mechanics of Space Systems, Reston, VA: AIAA Education Series, 2014.

[11] W. Dixon, M. S. de Queiroz, D. M. Dawson and F. Zhang, "Tracking Control of Robot Manipulators with Bounded Torque Inputs," *Robotica,* vol. 17, pp. 121-129, 1999.

[12] I. Harris and W. Priester, "Time-Dependent Structure of the Upper Atmosphere," *Journal of the Atmospheric Sciences,* vol. 19, no. 4, pp. 286-301, 1962.

Authorized licensed use limited to: Florida Institute of Technology. Downloaded on March 03,2025 at 15:46:48 UTC from IEEE Xplore. Restrictions apply.